

Top Partner Discovery in the $T \rightarrow tZ$ channel at the LHC

Jürgen Reuter and Marco Tonini

DESY Theory Group

Notkestr. 85, D-22607 Hamburg, Germany

E-mail: juergen.reuter@desy.de, marco.tonini@desy.de

ABSTRACT: In this paper we study the discovery potential of the LHC run II for heavy vector-like top quarks in the decay channel to a top and a Z boson. Despite the usually smaller branching ratio compared to charged-current decays, this channel is rather clean and allows for a complete mass reconstruction of the heavy top. The latter is achieved in the leptonic decay channel of the Z boson and in the fully hadronic top channel using boosted jet and jet substructure techniques. To be as model-independent as possible, a simplified model approach with only two free parameters has been applied. The results are presented in terms of parameter space regions for 3σ evidence or 5σ discovery for such new states in that channel.

KEYWORDS: LHC phenomenology, Top Partners, Boosted-top tagging, Simplified model approach, Little Higgs models, Composite Higgs models

ARXIV EPRINT: [1409.6962](https://arxiv.org/abs/1409.6962)

Contents

1	Introduction	1
2	Top partners and top tagging	3
2.1	Models comprising top partners	3
2.2	Simplified model approach	7
2.3	Tagging the boosted regime	7
3	Setup of the analysis	8
3.1	Event generation	8
3.2	Reconstruction of physics objects	10
3.3	Cutflow	11
4	Results	16
5	Conclusion	19

1 Introduction

With the advent of the Large Hadron Collider (LHC), a whole new range of energies is opening up for experimental particle physics, namely the range from the electroweak scale v up to the multi-TeV regime. Within the first 2010-2012 run of the LHC crucial results have been already collected, most notably the discovery of a (light) Higgs boson with mass $m_h \sim 125$ GeV, publicly announced on the 4th of July 2012 [1, 2]. Also remarkable are the (preliminary) measurements of the Higgs couplings and production modes, which are turning out to be as predicted by the Standard Model: no significant sign of new phenomena has been observed so far. This is starting to provide severe constraints on possible theories that differ significantly from the Standard Model at the probed energies.

Despite this enormous success, we know that the Standard Model cannot describe all phenomena we have observed so far. In particular, the absence of a possible candidate to describe the Dark Matter and Dark Energy hinted by various cosmological and astrophysical observations as well as the missing CP violation for the explanation of the baryon-antibaryon asymmetry represent the main experimental results that cannot be accommodated within the SM.

Furthermore, different theoretical motivations are considered as issues of the actual Standard Model formulation above the electroweak scale. The most notable one is the fine-tuning problem: a light (fundamental) Higgs boson implies large accidental cancellations between different and in principle uncorrelated physical quantities, due to its large radiative sensitivity to possible higher scales in the theory. In a “natural” theory, large cancellations among uncorrelated terms should either not be present, or explained by means of symmetry arguments.

The issue of a necessary fine-tuning to account for a light Higgs boson has always been the main guideline for possible model building of Beyond the Standard Model (BSM) Physics: suitable new

phenomena should appear around the TeV energy scale in order to suppress the large radiative corrections to the Higgs mass. The most sought-after solution of the fine-tuning problem at the LHC is Supersymmetry (SUSY). An alternative solution is given by strongly-coupled extensions of the Standard Model. In this class of models, a new strong interaction sector is assumed at some energy above the electroweak scale, making the Higgs a composite object below the compositeness scale. Since it does not make sense to speak of an elementary scalar Higgs boson above the compositeness scale, at low energies the Higgs mass is thus at most sensitive to the value of the compositeness scale. In this sense, assuming a strong sector as UV-completion of the Standard Model prevents dangerous fine-tuning requirements to account for the observed Higgs mass. However, in a generic strongly interacting extension of the Standard Model, the compositeness scale would be close to the Higgs mass, causing a conflict with electroweak precision observables and direct searches for heavy resonances.

A consistent way to implement a strongly coupled UV-completion of the Standard Model has led to models in which the Higgs arises as pseudo-Goldstone boson of some spontaneously broken global symmetry of the strong sector at a scale $f \gg v$. The Higgs boson can thus be much lighter than other possible states of the composite sector, in complete analogy with the low-energy QCD description, where the pions arise as a set of scalar states naturally lighter than the compositeness scale Λ_{QCD} , with all other resonances at higher masses. These models are generically called Composite Higgs models.

In particular, light partners of the SM top are a key ingredient for the naturalness argument of different BSM models, in order to cut off the quadratic UV-sensitivity of the Higgs mass squared parameter from SM top loops. This is a common feature for generic Supersymmetric and Composite Higgs models. The main difference between supersymmetric top partners (*stops*) and top partners arising in strongly coupled models is their different spin, spin 0 vs. spin 1/2, respectively. The fermionic top partners are usually vector-like particles.

Contrary to sequential fourth-generation quarks, which are heavily constrained already from Higgs boson searches, since they would yield a large impact e.g. in the one-loop induced processes like gluon fusion production and diphoton decay of the Higgs, indirect bounds on vector-like quarks are much weaker. Their effect on the Higgs observables is indeed less dramatic than fourth generation quarks as their vector-like nature allows to obtain a large Dirac mass without introducing a large Yukawa coupling to the Higgs.

Both the ATLAS and CMS collaborations have recently performed dedicated searches for top partners [3–10]. Depending on the particular branching ratio under investigation, the actual limits on the top partner mass, at $\sqrt{s} = 8$ TeV and with up to 20 fb^{-1} of integrated luminosity, do not exceed $700 - 800$ GeV. Most of these experimental searches assume the new heavy quarks to be pair produced: however, searches combining pair production with single production through electroweak interactions will become an important feature in the future. Present limits from the LHC start to enter the region in which single production becomes comparable to pair production due to the smaller phase space suppression, even if an electroweak coupling is involved.

Many different theoretical analyses involving top partners have been recently proposed, some of them exploiting tagging techniques [11–30]. However, a closer look to these references reveals that the top partner decay $T \rightarrow Z t$ has not been thoroughly explored yet, because it appears rather difficult at first glance. In particular, the all-hadronic final state suffers from huge SM backgrounds, making the alternative $T \rightarrow W b$ channel more suited for all-hadronic analyses due to the enhanced branching ratio and the possibility to exploit b-tagging. Furthermore, the channel

involving a leptonic decay of the Z entails a large suppression from the Z leptonic branching ratio, $\text{BR}(Z \rightarrow \ell^+ \ell^-) \sim 0.067$ ($\ell \equiv e, \mu$). A study of the $T \rightarrow Z t$ “trilepton” channel with both leptonic decays of the Z boson and top quark has been first proposed in [24] and recently published in [30].

In order to test the nature of the top partner, it is important to develop search strategies which might cover all possible channels, especially for the foreseen LHC energy upgrade to 13 TeV. For this reason, we develop a search strategy tailored for a charge-2/3 top partner optimised for its decay channel $T \rightarrow t Z \rightarrow (q q' b) (\ell^+ \ell^-)$, at the LHC with center-of-mass energy of $\sqrt{s} = 13$ TeV and integrated luminosity of 300 fb^{-1} . We present, with minimal assumptions on the underlying model, a method to discover a possible top partner signature with large statistical significance. More importantly, we aim at a precise measurement of its invariant mass.

Recently, ATLAS presented a $\sqrt{s} = 8$ TeV search [3, 4] optimised for either pair or single production of a top partner, subsequently decaying as $T \rightarrow Z t$ with leptonic decay of the Z boson. This encouraged us to further analyse this rather unexplored process, in order to provide an effective search strategy for the forthcoming 13 TeV LHC runs.

The structure of the paper is the following. In section 2 we briefly review different examples of models comprising top partners in the context of strongly coupled UV-completions of the SM. This is followed by a discussion of a simplified-model approach for the simulation of top partner signal events, and some details about top-tagging techniques useful to tag the boosted regime of the top partner decay products. Section 3 presents the setup of our proposed analysis, namely the event generation procedure, the reconstruction of physics objects, and the definition of the dedicated selection cuts. Finally, a thorough discussion of the results is presented in section 4, together with concluding remarks in section 5.

2 Top partners and top tagging

2.1 Models comprising top partners

All differences on the underlying top-partner model depend on the choice of the representation of the new quarks and on the assignment of the quantum numbers. We will briefly discuss some examples of top partners in the context of strongly coupled UV-completions of the SM.

A prominent class of models predicting light spin-1/2 vector-like top partners is the class of Composite Higgs models [16, 31–37]. In the minimal Composite Higgs scenario, the coset structure is $SO(5)/SO(4)$. The main guiding principle is that the decays and single production of the new partners are generated via mixing with the standard quarks, induced by Yukawa interactions with the Higgs. In particular, only the right-handed SM top quark t_R is promoted to a fully composite state belonging to a complete multiplet (singlet) of the unbroken $SO(4)$ group, while the (elementary) left-handed SM doublet q_L is assumed to be embedded into an incomplete $SO(5)$ multiplet and to couple linearly to the strong sector.

The vector-like top partners are introduced as composite bound states belonging to a complete multiplet Ψ of the unbroken group $SO(4)$: two cases are usually considered, namely $\Psi \sim \mathbf{4}$ or $\Psi \sim \mathbf{1}$ under $SO(4)$. We will refer to these two implementations as M_{45} and M_{15} , respectively. In the M_{45} case, the multiplet Ψ includes two charge-2/3 top partners $X_{2/3}$, T , one exotic charge-5/3 top partner $X_{5/3}$, and a charge-1/3 bottom partner B : under the SM gauge group, the four

components of Ψ decompose into two SM doublets (T , B) and ($X_{5/3}$, $X_{2/3}$) of hypercharge 1/6 and 7/6, respectively. In the $M1_5$ case, only one $SU(2)$ -singlet charge-2/3 top partner \tilde{T} is introduced.

Assuming an embedding of the elementary SM doublet q_L into an incomplete fundamental representation $Q_L^5 \sim \mathbf{5}$ of $SO(5)$, the following interactions involving the top partners can be written down [16]:

$$\mathcal{L}^{M4_5} \supset i c_1 (\bar{\Psi}_R)_i \gamma^\mu d_\mu^i t_R + y f (\bar{Q}_L^5)^I U_{Ii} \Psi_R^i + y c_2 f (\bar{Q}_L^5)^I U_{I5} t_R + \text{h.c.} \quad (2.1)$$

$$\mathcal{L}^{M1_5} \supset y f (\bar{Q}_L^5)^I U_{I5} \Psi_R + y c_2 f (\bar{Q}_L^5)^I U_{I5} t_R + \text{h.c.} \quad (2.2)$$

In particular, d_μ is the connection symbol defined in the CCWZ formalism [38, 39], U is the 5×5 Goldstone boson matrix, y is a Yukawa coupling controlling the mixing between the composite and elementary states, c_1, c_2 are $\mathcal{O}(1)$ parameters associated with the interactions of t_R , and f is the usual symmetry breaking scale of the strong sector. For the model $M1_5$, a direct coupling of Ψ with t_R like the first term in eq. (2.1) can be removed with a field redefinition. Note that the operators proportional to y explicitly break the $SO(5)$ symmetry, since q_L is embedded into an incomplete $SO(5)$ multiplet, giving rise to the leading contribution to the Higgs potential triggering the electroweak symmetry breaking.

It turns out that the couplings of the top partners to the Goldstone bosons (ϕ^\pm, ϕ^0), which in the high energy limit correspond to the longitudinal components of the gauge bosons (Equivalence Theorem), and to the Higgs h , are proportional to linear combinations of the couplings y, c [16]:

$$M4_5 : \begin{cases} \phi^+ \bar{X}_{5/3L} t_R & : \sqrt{2} c_1 g_\Psi \\ (h + i\phi^0) \bar{X}_{2/3L} t_R & : c_1 g_\Psi \\ (h - i\phi^0) \bar{T}_L t_R & : -c_1 \sqrt{y^2 + g_\Psi^2} + \frac{c_2 y^2}{\sqrt{2} \sqrt{y^2 + g_\Psi^2}} \\ \phi^- \bar{B}_L t_R & : c_1 \sqrt{2} \sqrt{y^2 + g_\Psi^2} - \frac{c_2 y^2}{\sqrt{y^2 + g_\Psi^2}} \end{cases} \quad (2.3)$$

$$M1_5 : \begin{cases} (h + i\phi^0) \bar{\tilde{T}}_R t_L & : \frac{y}{\sqrt{2}} \\ \phi^+ \bar{\tilde{T}}_R b_L & : y, \end{cases} \quad (2.4)$$

where $g_\Psi = M_\Psi/f$, M_Ψ being the Dirac mass of the top partner multiplet.

These couplings govern the associated production of the different top partners. In particular we see that the $SU(2)$ -singlet top partner \tilde{T} can be copiously produced in association with a b-quark: from eq. (2.4), its coupling to the W boson is given by

$$\left(\frac{m_W}{M_{\tilde{T}}} \right) \cdot \text{coeff}(\phi^+ \bar{\tilde{T}}_R b_L) = \left(\frac{m_W}{M_{\tilde{T}}} \right) y \equiv \frac{g g^*}{\sqrt{2}}, \quad (2.5)$$

with y of order $\mathcal{O}(1)$ to reproduce the SM top mass.

Furthermore, we can easily read off from eq. (2.3) and (2.4) the different branching ratios of all top partners. For example, in the decoupling limit of $m_\Psi \rightarrow \infty$, the branching ratios of the $M1_5$ $SU(2)$ -singlet top partner \tilde{T} are

$$\begin{aligned} BR(\tilde{T} \rightarrow W b) &\sim 0.5, \\ BR(\tilde{T} \rightarrow Z t) &\sim 0.25, \\ BR(\tilde{T} \rightarrow h t) &\sim 0.25, \end{aligned} \quad (2.6)$$

while the branching ratios of the charge-2/3 top partners of M_{45} are given by

$$\begin{aligned} BR(X_{2/3} \rightarrow Z t) &\sim BR(T \rightarrow Z t) \sim 0.5, \\ BR(X_{2/3} \rightarrow h t) &\sim BR(T \rightarrow h t) \sim 0.5. \end{aligned} \quad (2.7)$$

Besides the composite Higgs models, there are other models predicting an $SU(2)$ -singlet top partner, e.g. Little Higgs models. A prime example is the Littlest Higgs Model with T-parity (LHT) [40–42]. Within the class of strongly coupled UV-completions of the SM, Little Higgs models represent an appealing realisation exploiting a natural separation between the electroweak scale v and the compositeness scale $\Lambda = 4\pi f$. This is realised through Collective Symmetry Breaking. This mechanism forces the global symmetries, preventing the generation of a Higgs mass term, to be broken by at least two operators: in this way, the Higgs mass-generating one-loop diagrams are at most logarithmically divergent in Λ , while quadratically divergent only at two-loop level. The realisation of this mechanism requires the introduction of additional partner fields in the scalar, vector boson and top sectors, in order to formulate “collective” couplings of the Higgs boson to the SM particles and their respective partners.

The Littlest Higgs model is based on a non-linear sigma model describing the global spontaneous symmetry breaking at the scale $f \sim \mathcal{O}(\text{TeV})$

$$SU(5)/SO(5). \quad (2.8)$$

The mechanism for this symmetry breaking is not specified: the model describes an effective theory valid up to the compositeness scale $\Lambda = 4\pi f$, where a strong sector as UV-completion is assumed. For comprehensive reviews of the model details see [43–48]. In here we just mention that, in addition to the SM particles, new charged heavy vector bosons (W_H^\pm), a neutral heavy vector boson (Z_H), a heavy photon (A_H), a top partner (T_+) and a triplet of scalar heavy particles (Φ) are present: these heavy particles acquire masses of order f from the $SU(5)/SO(5)$ spontaneous breaking. Couplings of the Higgs to these particles radiatively generate a potential for the Higgs boson, triggering the electroweak symmetry breaking.

As the original Littlest Higgs model suffers from severe constraints from electroweak precision tests (EWPT), which could be satisfied only in rather extreme regions of the parameter space [49–51], these can be evaded with the introduction of a custodial symmetry, ungauging some of the symmetries [52, 53], or with the introduction of a conserved discrete symmetry called T-parity [41, 42]. Using the latter, the scale f can be as low as $\mathcal{O}(500 \text{ GeV})$, resulting in a rather low amount of fine-tuning to accommodate the observed Higgs mass, together with not too suppressed production cross sections of new particles [45, 51, 54, 55].

Recent studies including constraints from EWPT, Higgs observables and results from direct searches for new particles, have set a lower bound on the scale f to be [51, 56, 57]

$$(f_{\text{LHT, A}})_{\text{EWPT+Higgs}} \gtrsim 694 \text{ GeV} \quad (2.9)$$

$$(f_{\text{LHT, B}})_{\text{EWPT+Higgs}} \gtrsim 560 \text{ GeV}, \quad (2.10)$$

depending on the particular implementation of the down Yukawa couplings. The latter translate into e.g. a lower bound on the mass of the top partner

$$(M_{T_+})_{\text{LHT, A}} \gtrsim 975 \text{ GeV} \quad (2.11)$$

$$(M_{T_+})_{\text{LHT, B}} \gtrsim 787 \text{ GeV}. \quad (2.12)$$

Besides the (T-even) top partner T_+ , which is introduced to regularise the quadratic divergence of the Higgs mass from the SM top loop, a consistent implementation of T-parity in the top sector requires the introduction of a T-odd counterpart of the heavy top partner, called T_- , and a T-odd partner of the (T-even) SM top, called t_H . While the introduction of the former is specific for the top sector, every SM fermion is instead required to possess a T-odd partner, generically called mirror fermion. Both T_+ and T_- acquire a mass of order f from a Yukawa-like Lagrangian, as well as the SM top after electroweak symmetry breaking; on the other hand, the mass generation for mirror fermions requires the introduction of a Lagrangian involving couplings proportional to a new free parameter κ . R is a ratio of Yukawa couplings in the top sector (for more details, cf. e.g. [51]).

Particle	Decay	BR $_{\kappa=1.0}$	BR $_{\kappa=0.4}$
d_H	$W_H^- u$	63%	0%
	$Z_H d$	31%	0%
	$A_H d$	6%	100%
u_H	$W_H^+ d$	61%	0%
	$Z_H u$	30%	0%
	$A_H u$	9%	100%
T_+	$W^+ b$	46%	46%
	$Z t$	22%	22%
	$H t$	21%	21%
	$T_- A_H$	11%	11%
T_-	$A_H t$	100%	100%

Table 1. Overview of the decay modes with the corresponding branching ratios of the LHT new quarks, with reference values $f = 1$ TeV and $R = 1.0$ [56, 57]. We emphasise two possible scenarios, namely with the mirror quarks q_H either lighter ($\kappa = 0.4$) or heavier ($\kappa = 1.0$) than the gauge boson partners. The heavy leptons decay analogously to the heavy quarks and the decays involving generic up or down quarks have to be considered as summed over all flavours.

In table 1 we list an overview of decay modes and branching ratios of the LHT new particles, with reference values $f = 1$ TeV and $R = 1.0$. In particular, the LHT T_+ top partner shares the 2:1:1 ratio for the decays into SM particles as in eq. (2.6), but allows for a further decay channel involving the T-odd partner T_- and the heavy photon A_H with a non-negligible rate.

The electroweak coupling of T_+ to the W boson, which governs its associated production with a b-quark, is given by [48]

$$\text{coeff}(W^+ \bar{T}_{+R} b_L) = \frac{g}{\sqrt{2}} \frac{R^2}{1+R^2} \frac{v}{f} + \mathcal{O}\left(\frac{v^2}{f^2}\right) \equiv \frac{g g^*}{\sqrt{2}}. \quad (2.13)$$

Note that we again put this into the same form as eq. (2.5).

From this, it is clear that charge-2/3 vector-like top partners share similar final state topologies, with different branching ratios and single production couplings depending on the particular underlying model. Therefore, when looking for possible dedicated searches for top partners at the LHC, it is favourable to use simplified model approaches, involving for example only the mass of the top partner and its “single production” coupling as free parameters. We pursue this approach for the rest of the paper.

2.2 Simplified model approach

Recently, a generic parametrisation of an effective Lagrangian for top partners has been proposed in [58], where the authors considered vector-like quarks embedded in different representations of the weak $SU(2)$ group, with other minimal assumptions regarding the structure of the couplings. In particular, vector-like quarks which can mix and decay directly into SM quarks of all generations are included. Particularly interesting for our purposes is the case in which the top partner is an $SU(2)$ singlet, with couplings only to the third generation of SM quarks. The Lagrangian parametrising the possible top partner interactions reads [58]

$$\mathcal{L}_T \supset \frac{g^*}{\sqrt{2}} \left[\frac{g}{\sqrt{2}} \bar{T}_L W_\mu^+ \gamma^\mu b_L + \frac{g}{2c_W} \bar{T}_L Z_\mu \gamma^\mu t_L - \frac{M_T}{v} \bar{T}_R h t_L - \frac{m_t}{v} \bar{T}_L h t_R \right] + \text{h.c.}, \quad (2.14)$$

where M_T is the top partner mass, and g^* parametrises the single production coupling in association with a b- or a top-quark. In the limit of $M_T \gg m_t$, the width of the top partner is

$$\Gamma_T \simeq \frac{(g g^*)^2}{64 \pi m_W^2} \left(1 + \frac{1}{2} + \frac{1}{2} \right), \quad (2.15)$$

where the three contributions in parentheses arise from the top partner decays to W , Z and Higgs, respectively. The different branching ratios of T are thus clearly the same as in eq. (2.6), since we are describing effectively the same type of top partner as in M_{15} .

For our proposed top partner search at the LHC we will exploit a simplified-model approach, assuming the interactions described by the Lagrangian of eq. (2.14), where the only free parameters will be the top partner mass M_T and its “single production” coupling g^* . In this way, our results will be straightforwardly mapped within the context of the M_{15} minimal Composite Higgs model, namely by identifying as in eq. (2.5)

$$y = \frac{g g^*}{\sqrt{2}} \frac{M_{\tilde{T}}}{m_W} \quad (M_{15}). \quad (2.16)$$

For comparison, with $y = 1$ and $M_{\tilde{T}} = 1 \text{ TeV}$ one obtains $g^* \sim 0.17$.

On the other hand, while an immediate map of g^* to the LHT parameters is straightforward from eq. (2.13), namely with

$$g^* = \sqrt{2} \frac{R^2}{1 + R^2} \frac{v}{f} + \mathcal{O}\left(\frac{v^2}{f^2}\right) \quad (\text{LHT}), \quad (2.17)$$

the Lagrangian of eq. (2.14) does not exactly reproduce the T_+ phenomenology because of the absence of the $T_+ \rightarrow T_- A_H$ vertex in the simplified-model approach. In particular, it should be kept in mind that the different branching ratios of the top partner described by eq. (2.14) slightly overestimate the actual branching ratios of the LHT T_+ partner. For comparison, fixing $R = 1.0$ and $f = 1 \text{ TeV}$ yields $g^* \sim 0.17$.

Finally, by using the simplified-model approach, we also underestimate the branching ratios of the charge-2/3 top partners within the M_{45} model, given in eq. (2.7): our results will be conservative in this case.

2.3 Tagging the boosted regime

Let us now focus on the kinematics of a possible top partner decay. For masses much heavier than the top quark, the top partner decay products are produced with large spatial separation (back-to-back decay). Furthermore, for large center-of-mass energies, these primary top partner decay

products are necessarily boosted, namely with transverse momentum p_T which considerably exceeds their rest mass: this means that the subsequent decay products are highly collimated in one area of the detector. As a rule of thumb, the decay products of a highly boosted particle of mass m and transverse momentum $p_T \gg m$ are collimated within a cone of radius

$$\Delta R \sim 2 \frac{m}{p_T}, \quad (2.18)$$

such that e.g. the hadronic decays of a boosted SM top with $p_T \sim 250$ GeV are collimated within a detector region of radius $\Delta R \lesssim 1.4$.

In this kinematical regime, conventional reconstruction algorithms that rely on a jet-to-parton assignment are often not feasible. Crucial ingredients for high center-of-mass searches involving massive particles are the so-called substructure methods [59, 60], to identify the top partner decay products within large “fat” jets. Generically, focusing on hadronic decays of boosted objects, these substructure methods first reconstruct jets with a much larger radius parameter, in order to capture the energy of the complete hadronic decay in a single jet; then use method-dependent discriminating variables to analyse the internal structure of the fat jets, to separate boosted objects from the large QCD background.

Jet-substructure methods which are dedicated to the identification of possible boosted tops are generically called *top-taggers*. In particular, top tagging techniques are crucial not only to reduce the huge SM QCD and $t\bar{t}$ backgrounds, exploiting the particular kinematical feature of the boosted decay products, but also to avoid combinatorics in the reconstruction of the top four momentum from high multiplicity final-state jets. In this way, fully-hadronic top decays with a larger branching ratio compared to leptonic final states, can be systematically exploited for searches involving top partners. A review on top-taggers can be found e.g. in [61].

It turns out, see e.g. refs. [6, 25], that the Heidelberg-Eugene-Paris top-tagger [60] (“HEPTopTagger”) can have a relatively better performance compared to other algorithms, especially for moderately boosted tops. For this reason, in our analysis we will adopt the HEPTopTagger to tag boosted top quarks in the considered signal events.

3 Setup of the analysis

3.1 Event generation

As mentioned in section 2, we investigate processes involving a charge-2/3 vector-like top partner T , inclusively pair and associated produced, with subsequent decay

$$T \rightarrow t Z \rightarrow (q q' b) (\ell^+ \ell^-). \quad (3.1)$$

The process is depicted in figure 1 together with our conditions on the cones of the boosted objects to be defined below. We study a possible search strategy optimised for the LHC with center-of-mass energy of $\sqrt{s} = 13$ TeV and integrated luminosity of 300 fb^{-1} . The clean final state and the absence of missing transverse energy makes this channel promising for a possible mass reconstruction of the top partner, even if the possible SM backgrounds are rather huge.

Signal and background events have been simulated using MadGraph5 v2.1 [62], and Pythia 8.183 [63] for parton-shower and fragmentation, and further analysed via Delphes 3.1 [64] for a fast detector simulation following the specifications which we are going to detail in the following. All cross

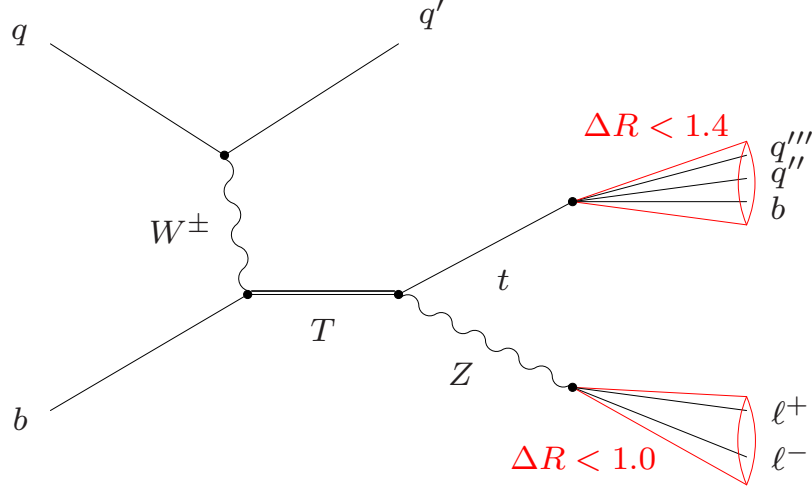


Figure 1. Single production of a heavy top partner T with subsequent decay into tZ . The boosted decay products of the latter are collected inside cones of $\Delta R < 1.4$ and $\Delta R < 1.0$, respectively.

sections have been checked with WHIZARD v2.2 [65–67]. In particular, an anti- k_t jet clustering algorithm with radius parameter of $R = 0.4$ is used to reconstruct jets, which in the following we will call *slim jets*. The same Pythia output is simultaneously analysed through FastJet 3.0.6 [68, 69] in order to cluster the hadronic activity using the Cambridge-Aachen algorithm with larger radius parameter of $R = 1.5$, reconstructing jets which in the following we will identify as *fat jets*.

The model file generating signal events according to the Lagrangian of eq. (2.14) [58], can be found in the dedicated FeynRules model database webpage (“Singlet T Model VLQ”) [70–72]. The corresponding free parameters are the top partner mass M_T , the coupling g^* which governs the top partner single production involving a t-channel W , and the rate R_L of T decays into light quarks. We fix $R_L = 0$ in order to force T to decay only to third generation SM quarks. For our analysis we consider values in the range

$$M_T \in [850, 1450] \text{ GeV}, \quad g^* \in [0.05, 0.5]. \quad (3.2)$$

In particular, our signal processes consist of pair and associated production of a charge-2/3 vector-like top partner T , with subsequent decay as in eq. (3.1): in the case of pair production we consider the inclusive decay of the second top partner according to the branching ratios reported in eq. (2.6). The LO signal cross section is calculated via MG5, depending on the particular choice of the free parameters which were consistently updated, together with the top partner width, before the event generation. We further rescale the signal cross section with a K-factor which we evaluate using Hathor 2.0 [73, 74]. In particular, we calculate the K-factors for both top pair (NNLO) and single productions (NLO) for different values of the top mass in the range (3.2), eventually choosing a minimal and hence conservative value of $K = 1.14$.

The main SM background processes turn out to be Z + jets, associated Z production with a pair of top quarks ($t\bar{t}Z$ + jets), plus subleading contributions from associated Z production with single top ($t/\bar{t}Z$ + jets). All other potentially dangerous contributions like $t\bar{t}$ + jets, $t\bar{t}W^\pm$ + jets and $\gamma^* \rightarrow \ell^+\ell^-$ + jets turn out to be negligible by requiring exactly two opposite charge and same flavour leptons in the final state with invariant mass satisfying $|m_{\ell^+\ell^-} - m_Z| < 10 \text{ GeV}$. Furthermore, the large $W^\pm Z$ + jets background becomes also negligible due to the smaller boost of the Z boson

compared to the signal and the backgrounds involving the top quark, and by exploiting b- and top-tagging.

Large samples of background events are generated using MG5, requiring up to three, two or one additional hard jets at matrix element level for $Z + \text{jets}$, $t/\bar{t} Z + \text{jets}$ and $t\bar{t} Z + \text{jets}$ processes, respectively. To avoid double counting of jets generated at matrix element level and jets radiated during the parton showering process, a CKKW-L merging procedure [75–77] is exploited. In particular we interface, for each background sample, the corresponding parton level MG5 outputs with different multiplicities of additional jets to Pythia 8.183 and its internally built-in routines for the CKKW-L merging, accordingly setting the merging scale value and the number of additional jets available from matrix element. This procedure guarantees a correct prediction for the (merged) cross section of the desired process.

bkg. process	K-factor	Ref.
$Z + \text{jets}$	1.20	[78]
$t\bar{t} Z + \text{jets}$	1.30	[79]
$t Z + \text{jets}$	1.11	[80]
$\bar{t} Z + \text{jets}$	1.09	[80]

Table 2. K-factors of the leading SM background processes for our analysis.

We rescale the evaluated background cross sections with appropriate K-factors from the corresponding publications, summarising the values in table 2. It should be noted that the inclusive $t\bar{t} Z + \text{jets}$ K-factor as given in [79] is $K = 1.39$: however, this value is reduced for large top transverse momenta, as in our case. For this reason we conservatively set $K = 1.30$ as in table 2.

3.2 Reconstruction of physics objects

Final state object reconstruction is performed mainly following the specifications detailed in [81]. An electron candidate is required to have a transverse momentum $p_T^e \geq 20 \text{ GeV}$ and $|\eta^e| < 2.47$. An isolation requirement is further applied, namely the total p_T of all charged particles q satisfying $p_T^q > 1.0 \text{ GeV}$ and $\Delta R(e, q) < 0.3$, should be less than 10% of p_T^e . A muon candidate is required to satisfy $p_T^\mu \geq 10 \text{ GeV}$ and $|\eta^\mu| < 2.5$. The isolation for the muon requires that the total p_T of all charged particles q satisfying $p_T^q > 1.0 \text{ GeV}$ and $\Delta R(\mu, q) < 0.4$, should be less than 6% of p_T^μ .

As mentioned before, slim jets are clustered from all final state particles with $|\eta| < 4.9$, except isolated leptons and neutrinos, using the anti- k_t algorithm with a radius parameter of $R = 0.4$ as implemented in Delphes 3.1. Only slim jets with $p_T^j \geq 20 \text{ GeV}$ are further considered. Slim jets are possibly identified as b-jets through the built-in Delphes 3.1 dedicated routines: in particular, we set the probability to tag b-jets (b-tag efficiency) to 70%, together with a charm quark misidentification probability of 10%. Tagged b-jets are further required to be reconstructed within $|\eta^b| < 2.5$.

Fat jets are simultaneously clustered using FastJet 3.0.6 on the same final state particles with $|\eta| < 4.9$, except isolated leptons and neutrinos, using the Cambridge-Aachen algorithm with radius parameter of $R = 1.5$. Only fat jets with $p_T^j \geq 20 \text{ GeV}$ are further considered.

3.3 Cutflow

Events are required to contain in the final state at least two leptons with minimum transverse momentum $p_T^\ell > 25 \text{ GeV}$. Among all possible pairs of leptons, we require at least one pair to consist of opposite charge and same flavour leptons matching the invariant mass of the Z boson, namely such that the lepton-pair invariant mass $m_{\ell^+\ell^-}$ satisfies

$$|m_{\ell^+\ell^-} - m_Z| < 10 \text{ GeV}. \quad (3.3)$$

We further require that, for at least one pair, the separation $\Delta R = \sqrt{\Delta\phi^2 + \Delta\eta^2}$ between the two candidate leptons reconstructing the Z mass should satisfy

$$\Delta R(\ell^+, \ell^-) < \Delta R(\ell^+, \ell^-)_{\text{max}} = 1.0. \quad (3.4)$$

If more than one pair of leptons satisfies the previous requirements, we select the pair with invariant mass closest to the Z boson mass. This pair of leptons allows us to fully reconstruct the four-momentum of the candidate Z boson.

The cut of eq. (3.4) is particularly effective to suppress SM backgrounds containing a Z boson, since it captures the expected boosted kinematics of the Z boson from the top partner decay. According to eq. (2.18), we expect indeed highly collimated decay products from a boosted Z . On the other hand, SM processes do not provide a large transverse boost to the Z boson, guaranteeing a good discrimination power to eq. (3.4).

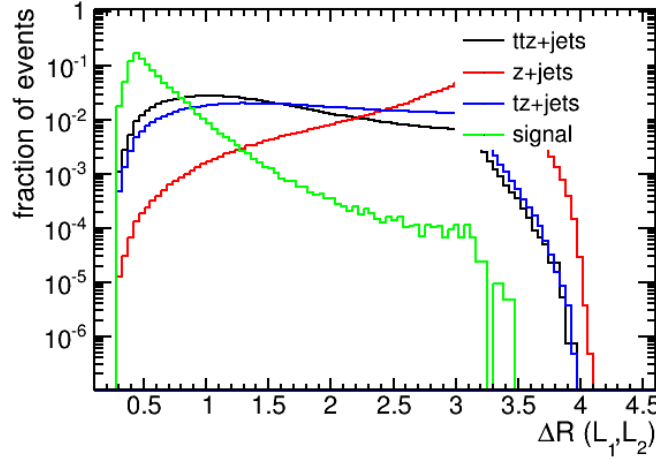


Figure 2. Distribution of the ΔR variable evaluated among candidate leptons reconstructing the Z boson for different processes. The signal process assumes $M_T = 1 \text{ TeV}$ and $g^* = 0.1$.

We show in figure 2 the distribution of the variable ΔR evaluated among candidate leptons reconstructing the Z boson, for the different background and signal processes: a peak at smaller values of ΔR is clearly visible for signal events. Note that the signal events used for all distribution plots shown in this section correspond to the benchmark point $M_T = 1 \text{ TeV}$ and $g^* = 0.1$.

Further kinematic constraints are imposed on the candidate Z boson, again to exploit the boosted properties of the considered signal. In particular, we require a large transverse momentum of the

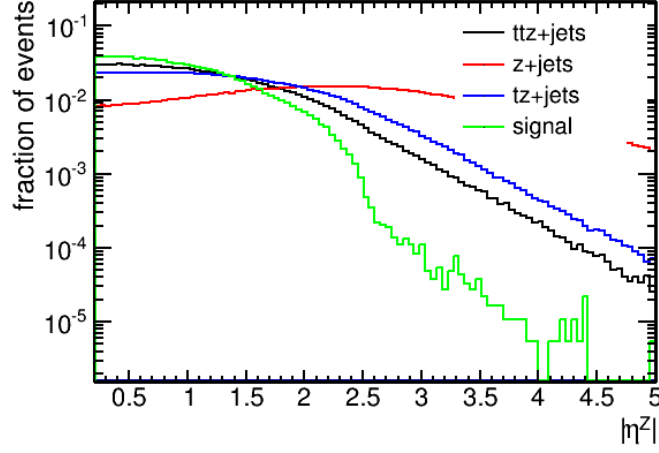


Figure 3. Distribution of the pseudorapidity $|\eta^Z|$ of the reconstructed candidate Z boson for different processes. The signal process assumes $M_T = 1$ TeV and $g^* = 0.1$.

candidate Z , namely

$$p_T^Z > p_{T,\min}^Z = 225 \text{ GeV}, \quad (3.5)$$

as well as requiring that the Z should be produced in the central region of the detector, namely with

$$|\eta^Z| < |\eta^Z|_{\max} = 2.3. \quad (3.6)$$

The requirement of eq. (3.6) is useful in rejecting e.g. the SM $Z + \text{jets}$ background, the latter being mostly produced via a Drell-Yan process with the initial quarks yielding a forward boost to the produced Z boson, as can be seen in figure 3.

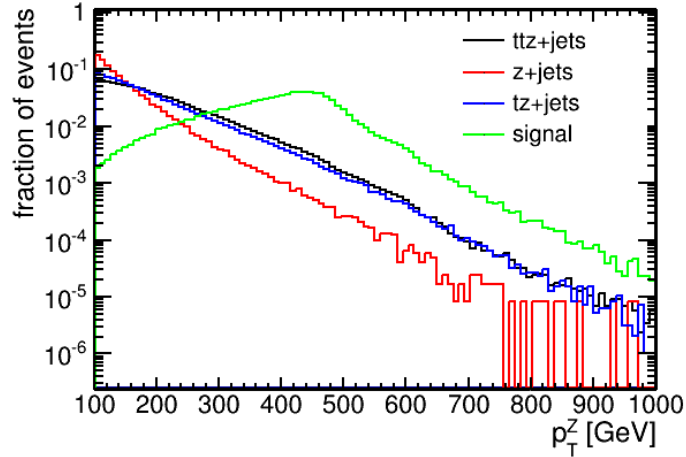


Figure 4. Distribution of the transverse momentum p_T^Z of the reconstructed candidate Z boson for different processes. The signal process assumes $M_T = 1$ TeV and $g^* = 0.1$.

In figure 4 we show the distribution of the transverse momentum of reconstructed Z boson candidates as described in the text. Larger transverse momenta are observed for the (boosted) Z from the signal process.

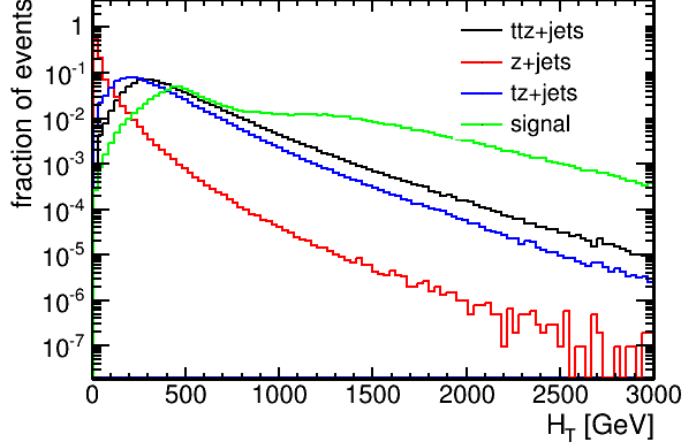


Figure 5. Distribution of the scalar sum of the transverse momenta H_T of the clustered *slim jets* for different processes. The signal process assumes $M_T = 1$ TeV and $g^* = 0.1$.

In the next step, the hadronic activity is considered for additional selection cuts. In order to account for the large boost of the top quark, we expect the final state jets to possess a large amount of transverse momentum. Therefore, we evaluate the H_T variable, namely the scalar sum of the transverse momenta of the reconstructed slim jets with $p_T^j > 30$ GeV and within $|\eta^j| < 3.0$, requiring each event to satisfy

$$H_T > H_{T, \min} = 400 \text{ GeV} . \quad (3.7)$$

In figure 5 we show the H_T distribution for the different considered processes. The signal distribution has a considerable tail for larger values of H_T compared to background events, confirming the good discrimination power of eq. (3.7). It is also worth noticing that the H_T distribution for the signal in figure 5 displays two different visible peaks, at $\mathcal{O}(500 \text{ GeV})$ and at $\mathcal{O}(1.3 \text{ TeV})$: these correspond to the top partner single and pair production components of the signal, respectively.

Among the reconstructed final state slim jets, we further require the presence of at least one tagged b-jet with

$$p_T^b > p_{T, \min}^b = 40 \text{ GeV} . \quad (3.8)$$

We then turn our attention to the reconstructed fat jets in the final state: our aim is to identify one reconstructed fat jet as our top candidate. At least one fat jet is required to be reconstructed among final state particles, satisfying the definition of fat jets given before, and with an additional requirement on its transverse momentum being

$$p_T^J > p_{T, \min}^J = 200 \text{ GeV} . \quad (3.9)$$

Most importantly, we require at least one fat jet to be HEPTop-tagged: the presence of a boosted SM top from the decay of a heavier resonance is indeed one of the main features of the signal. As

mentioned in section 2, top tagging is crucial not only as a discriminant against SM backgrounds, but also to effectively deal with the combinatorics in the top reconstruction from high multiplicity final state jets. If more than one fat jet is identified as a (boosted) top jet via the HEPTopTagger algorithm, we identify our candidate top as the fat jet mostly back-to-back with respect to the previously reconstructed candidate Z direction, as we would expect from the signal topology.

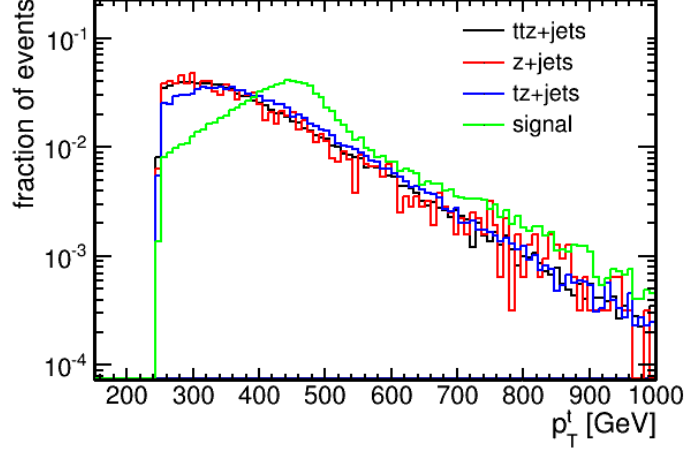


Figure 6. Distribution of the transverse momentum p_T^t of the reconstructed candidate top for different processes. The signal process assumes $M_T = 1$ TeV and $g^* = 0.1$.

To account for its boosted kinematics, we require that the transverse momentum of the candidate top should satisfy the cut

$$p_T^t > p_{T,\min}^t = 250 \text{ GeV}. \quad (3.10)$$

The p_T^t distribution of signal and background processes, after applying the cut of eq. (3.10), is shown in figure 6: a large fraction of signal events is observed for higher values of p_T^t .

Finally, to ensure that at least one of the tagged b-jets is originating from the candidate top, and not from additional radiation or as decay product of another involved particle, we require that the spatial separation between the candidate top and at least one of the slim jets tagged as b-jet should satisfy

$$\Delta R(t, b) < \Delta R(t, b)_{\max} = 0.8. \quad (3.11)$$

In other words, this cut ensures that at least one (slim) b-jet lies within the decay-cone of the candidate (fat jet) top.

To summarise the applied cuts, in table 3 we categorise them according to the reconstructed object on which they are applied. It should be noted that the actual values of $\Delta R(\ell^+, \ell^-)_{\max}$, $p_{T,\min}^Z$, $|\eta^Z|_{\max}$, $H_{T,\min}$, $p_{T,\min}^b$ are identified using an optimisation procedure: in particular, we scan the aforementioned cut values within appropriate ranges and evaluate the corresponding signal and background efficiencies for each possible configuration, obtaining a signal over background (S/B) map as a function of the cut values. We then identify the optimal cut configuration yielding the highest S/B ratio, assuming $M_T = 1$ TeV and $g^* = 0.1$ for the signal, and making sure that the total number of events after applying the cuts would remain reasonably large for 300 fb^{-1} of integrated luminosity.

selection cuts	
reconstructed Z	$n_{\ell^+\ell^-} \geq 1$ $ m_{\ell^+\ell^-} - m_Z < 10 \text{ GeV}$ $\Delta R(\ell^+, \ell^-) < 1.0$ $p_T^Z > 225 \text{ GeV}$ $ \eta^Z < 2.3$
slim jets	$H_T > 400 \text{ GeV}$ $n_b \geq 1, p_T^b > 40 \text{ GeV}$
fat jets	$n_J \geq 1, p_T^J > 200 \text{ GeV}$ $\text{HEPTop } n_t \geq 1$ $p_T^t > 250 \text{ GeV}$ $\Delta R(t, b) < 0.8$

Table 3. Summary of the selection cuts of the proposed analysis, sorted per type of reconstructed object on which the cut is applied.

selection cut	signal	$t\bar{t}Z + \text{jets}$	$tZ + \text{jets}$
$n_{\ell^+\ell^-}, m_{\ell^+\ell^-}, \Delta R(\ell^+, \ell^-)$	40.5%	9.0%	4.9%
$p_T^Z > p_{T,\min}^Z$	96%	69%	68%
$ \eta^Z < \eta^Z _{\max}$	99%	99%	99%
$H_T > H_{T,\min}$	80%	64%	61%
$n_b \geq 1, p_T^b > p_{T,\min}^b$	77%	72%	55%
$n_J \geq 1, p_T^J > p_{T,\min}^J$	99%	96%	97%
$\text{HEPTop } n_t \geq 1$	40%	36%	29%
$p_T^t > p_{T,\min}^t$	95%	82%	85%
$\Delta R(t, b) < \Delta R(t, b)_{\max}$	80%	67%	79%
final efficiency	7.4%	0.5%	0.2%
production cross section [pb]	$1.2 \cdot 10^{-3}$	$3.0 \cdot 10^{-2}$	$1.9 \cdot 10^{-2}$

Table 4. Efficiencies of the selection cuts evaluated on the considered processes. In particular, the signal events have been generated for the benchmark scenario $M_T = 1 \text{ TeV}$, $g^* = 0.1$.

In table 4 we collect the resulting efficiencies evaluated on the different processes, together with the corresponding production cross sections before the application of the cuts.

A final remark is devoted to possible pile-up effects, which we have not explicitly included in our analysis. It is expected that at the increased LHC center-of-mass energy runs and higher integrated luminosity, an average of more than 50 interactions per proton-bunch crossing will be observed. In particular, pile-up contamination might shift mass distributions to higher values and broaden them. Since its effect scales as the jet area, jets with larger cone area are more susceptible to pile-up contamination. A dedicated pile-up “mitigation” strategy is beyond the scope of our analysis, also because it would require a detailed detector information, but will certainly have to be taken into

account in a possible experimental analysis.

However, we expect our results to remain robust against pile-up effects, since our analysis mostly relies on the identification of leptons and exploits the HEPTopTagger to test the hadronic activity, with an effective soft-radiation rejection already built-in through a filtering procedure. In a recent publication [29] a thorough discussion has been presented of a possible search strategy for top partners including an estimation of pile-up effects: although being affected by pile-up contamination, the results of their analysis are still consistent.

4 Results

The procedure detailed in section 3 has a double benefit, namely largely improving the S/B ratio on one hand, and on the other hand uniquely determining the 4-momenta of the reconstructed top and Z boson candidates satisfying the possible kinematics of a top partner decay.

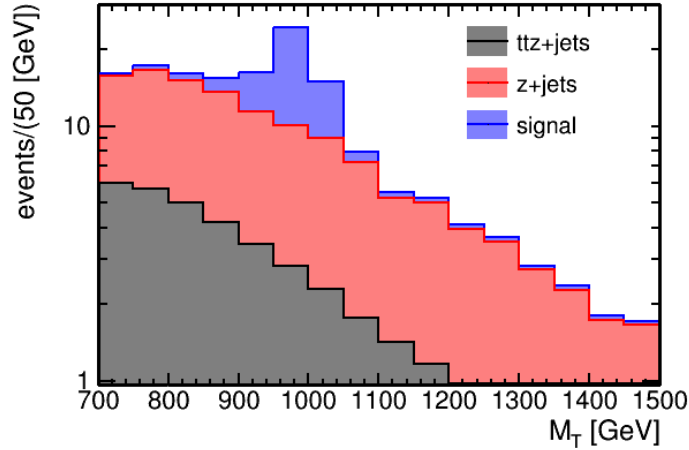


Figure 7. Stacked distribution plot of the invariant mass M_T of the reconstructed top partner for different processes. All distributions have been rescaled with the visible cross section of the corresponding processes, times an integrated luminosity of 300 fb^{-1} . The signal process assumes $M_T = 1 \text{ TeV}$ and $g^* = 0.1$. Other possible SM background processes are not shown in the plot since their contribution turned out to be negligible.

We finally plot the distribution of the invariant mass of the $(t-Z)$ system, which we expect to peak at the invariant mass of the on-shell top partner for the signal process, while described by a smoothly descending distribution for the different backgrounds, since the reconstructed top and Z in the latter events do not originate from an on-shell decay.

We show the result in figure 7, where we rescale the different distributions with the visible cross section of the corresponding processes, times an assumed integrated luminosity of 300 fb^{-1} . The different contributions are stacked in the plot. In this way, figure 7 shows a realistic amount of events which could be observed at the LHC with $\sqrt{s} = 13 \text{ TeV}$ and 300 fb^{-1} of integrated luminosity. For the signal we fixed $M_T = 1 \text{ TeV}$ and $g^* = 0.1$.

A peak in the bins around $M_T = 1$ TeV, fixing the bin width to 50 GeV, is clearly visible above the background distribution, with up to 25 total events in the most significant bin. The result of the analysis is therefore encouraging, and we support the experimental collaborations to further analyse the discussed channel: clearly, in a real experimental search the background estimation would be more robust and precise, e.g. via the inclusion of reconstructed fake leptons.

It is very important to estimate the significance of the signal peak above the SM background, in order to consistently claim the evidence for or the discovery of a top partner signal. In particular, the hypothesis testing procedure is carried out using the public BumpHunter code [82]. This code operates on datasets that are binned in some a-priori fixed set of bins: in our case, the input datasets correspond to the total number of signal+background and background-only events observed in M_T -bins of 50 GeV as in figure 7. The BumpHunter scans the input-given data using a window of varying width, and identifies the window with biggest excess compared to the background: the dedicated test statistic is designed to be sensitive to local excesses of data¹.

The same scanning procedure is further applied to pseudo-data sampled from the expectation of the background input², in order to reconstruct the “expected” distribution of the test statistic. The p -value of the test is calculated, being the probability that the test statistic will be equal to, or greater than the test statistic obtained by comparing the actual data to the background hypothesis. In other words, the p -value might be interpreted as a false-discovery probability. When the distribution of the test statistic is estimated using pseudo-experiments, as in our case, then the p -value is calculated as a binomial success probability.

An equivalent formulation in terms of Gaussian significance is straightforwardly obtained: it is common to claim that *evidence* for a new signal beyond the SM background is observed if the p -value of the peak corresponds to at least 3.0σ of Gaussian significance, while it is common to claim a *discovery* if the p -value corresponds to at least 5.0σ of Gaussian significance.

By running the BumpHunter on the datasets summarised in figure 7, the most significant peak is observed in the [900, 1050] GeV range, with an equivalent Gaussian significance of $2.6^{+1.0}_{-0.9}\sigma$. The uncertainties on the Gaussian significance of the peak are estimated by applying a 20% uncertainty on both the signal and background event yields, which might account for up to 30% possible further non-statistical uncertainties which we have not taken into account.

Different hypotheses on the underlying BSM signal would alter the shape of the signal distribution of figure 7. However, we expect that our analysis, although being optimised for the signal values $M_T = 1$ TeV and $g^* = 0.1$, should still display a peak in the M_T distribution even for different choices of the free parameters. In particular, a higher statistical significance of the peak might be achieved for different signal hypotheses. For this reason, we generate a grid of signal points for $M_T \in [850, 1450]$ GeV in steps of 150 GeV, and for $g^* \in [0.05, 0.5]$ in steps of 0.05, and for each combination we evaluate the corresponding significance of the peak, if observed.

Our results are displayed in figure 8, where regions of possible *evidence* (3.0σ) or *discovery* (5.0σ) of a top partner signal above the SM background are identified, assuming a dedicated LHC analysis as discussed in the text. Also shown are bands representing the effect of a possible total 30%

¹We setup the code to look for bumps in up to three consecutive bins, namely the possible mass resolution is at worst ± 75 GeV around the central value.

²In our case, we choose to model the background expectation by a Poisson distribution with the mean value distributed according to a Gamma distribution. The latter Gamma distribution is defined by fixing its mean value to the actual background bin value, and variance to the squared background bin error, as suggested in the BumpHunter manual. A total number of 10^8 pseudo-experiments is generated accordingly.

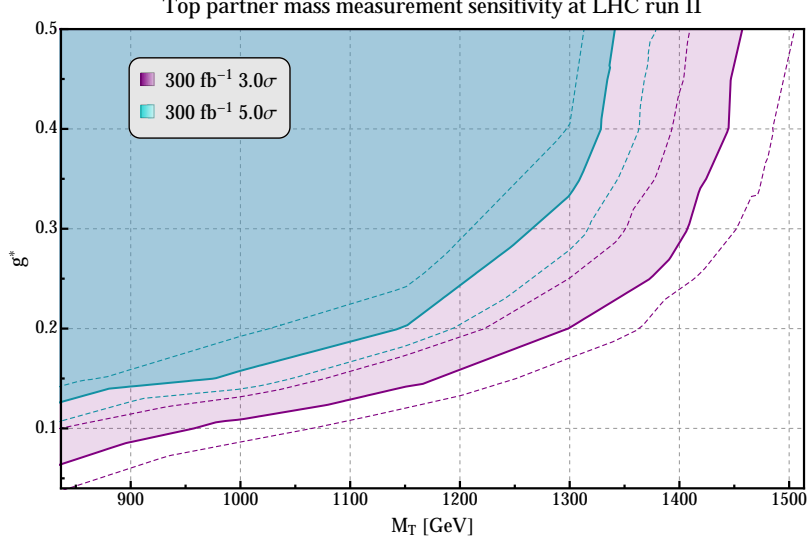


Figure 8. Parameter space regions of possible *evidence* (3.0σ) or *discovery* (5.0σ) of a top partner signal above the SM background, assuming the described analysis at the LHC with $\sqrt{s} = 13$ TeV and 300 fb^{-1} of integrated luminosity. Also shown are bands representing the effect of a possible further non-statistical 30% uncertainty on the visible cross section of the involved processes. If a signal peak is observed above the SM background, a possible mass measurement of the top partner invariant mass M_T is possible with a mass resolution of at worst ± 75 GeV around the central value.

uncertainty as discussed before. We observe that a large fraction of the considered parameter space might be probed using our proposed analysis; in particular, the top partner mass might be measured via the described BumpHunter procedure, with a mass resolution in our setup of at worst ± 75 GeV around the central value. The mass resolution might also be improved in a dedicated experimental setup.

From figure 8 we see that the signal is within the range of possible evidence for top partner masses up to roughly 1450 GeV with $g^* \lesssim 0.5$, while being still sensitive to g^* couplings down to 0.05 at lower masses. The $g^* \rightarrow 0$ limit corresponds to the pair-production only component, being a QCD process independent on the electroweak coupling: one can observe that within our hypotheses and analysis setup, the single production component has to be necessarily non-vanishing to guarantee a possible discovery potential of the signal, since no discovery reach is obtained for values of $g^* \lesssim 0.05$. Analogously, for fixed top partner mass, the discovery potential increases with g^* , since the single production cross section grows as $|g^*|^2$.

We can now compare the discovery reach as presented in figure 8 with other existing studies in literature. In particular, we can first compare with the results presented in [30], where the “trilepton” decay channel $T \rightarrow t Z \rightarrow (b \ell \nu) (\ell^+ \ell^-)$ has been scrutinised. In here, the authors considered a more general parameter space allowing mixing of the top partner with the other first two generations of quarks, namely letting the parameter R_L to be non vanishing: this way, the production cross section of the top partner dramatically increases due to parton distribution enhancement, and the discovery reach becomes highly sensitive to R_L . The highest significance has been observed for $R_L \sim 1$, corresponding to 50% mixing. The $R_L = 0$ case, as in our study, can be considered as the conservative case in which no flavour-changing coupling is introduced. By comparing the discovery reach obtained in [30] for $R_L = 0$ and 300 fb^{-1} of integrated luminosity, the trilepton and dilepton

analyses show very similar results: the trilepton analysis of [30] extends the reach by 200 – 300 GeV, probing possible top partner masses up to roughly 1700 GeV with $g^* \lesssim 0.5$, while being still sensitive to g^* couplings down to 0.1. Our dilepton search is instead more sensitive to lower values of the g^* coupling, namely down to $g^* \sim 0.05$ for top partner masses of 850 GeV. This is mainly due to the different b-jet cut requirement: while in the trilepton analysis exactly one b-jet is required to be identified, in our analysis we allow for the identification of more than one b-jet in the final state, being thus more efficient in tagging the pair production component of the signal.

Although not immediate due to the different parameter space definitions, we can also draw a comparison with other complementary studies for searches at the LHC run II involving a singlet top partner. In particular, in [26] the authors show that a mass reconstruction is possible within the $T \rightarrow th$ decay channel with 100 fb^{-1} of integrated luminosity at $\sqrt{s} = 14 \text{ TeV}$, proposing a search strategy optimised for two top partner mass points, namely $m_T = 800, 900 \text{ GeV}$, and assuming $\text{BR}(T \rightarrow th) = 1.0$. Furthermore, in [28] the authors project at $\sqrt{s} = 13 \text{ TeV}$ and 100 fb^{-1} of integrated luminosity the exclusion potential of the analysis first presented in [22], tailored for the leptonic $T \rightarrow Wb$ decay channel with $\text{BR}(T \rightarrow Wb) = 0.5$, obtaining an exclusion reach up to 2.0 TeV for single production if $c_L^{\text{Wb}} \gtrsim 0.4$. Analogously, in [27] the authors design a dedicated search strategy for the leptonic $T \rightarrow Wb$ decay channel, obtaining an expected exclusion reach for masses up to 1.0 TeV, including both pair and single production, with $\sqrt{s} = 14 \text{ TeV}$ and 30 fb^{-1} of integrated luminosity. Our analysis is thus competitive with the results of existing literature, and represents a viable and complementary candidate to pursue the search and mass measurement of a possible singlet top partner.

5 Conclusion

In this paper we have investigated the search for new vector-like heavy third-generation quarks, particularly top-like quarks in their decay channel into a top quark and a Z boson. Though this neutral-current decay channel has not been thoroughly investigated yet compared to the corresponding charged-current process into Wb or the decay into th , we believe that it is nevertheless worthwhile to look into it: firstly, it offers another independent search channel, and secondly the absence of missing transverse energy in the final state allows for a complete mass determination of the heavy top state. In order to be able to separate the fully hadronic top mode from the huge SM backgrounds, we applied the techniques of boosted objects and jet substructure to this channel.

Such heavy vector-like top partners appear in many different BSM models like models of (partial) compositeness, Little Higgs models, extra-dimensional models etc. In order to be as model-independent as possible we exploited a simplified model with only two free parameters, the heavy top mass and an electroweak coupling constant. We took both single and pair production of the heavy top quarks into account, where generally single production is the less phase-space constrained. The main SM backgrounds to these processes, $Z + \text{jets}$, $tZ + \text{jets}$ and $t\bar{t}Z + \text{jets}$ have been taken into account using known NLO K-factors. The boost of the leptonically decaying Z boson helps to suppress Drell-Yan backgrounds, while the signal is discriminated by the fat jet characteristics of the collimated decaying top quark.

To determine the sensitivity of the upcoming run II of LHC to such possible new states in this channel, we used the HepTopTagger to discriminate fat top quark jets from SM backgrounds on simulated events that have been merged with parton-shower generated QCD ISR and FSR jets. Afterwards, the fast detector simulation from Delphes has been used to assess efficiencies and un-

certainties from the cut-flow and the taggings. We briefly discussed possible pile-up contamination and further non-statistical uncertainties.

As a final result we gained the 3σ evidence reach as well as the 5σ discovery potential of LHC run II in the parameter plane of the two variables heavy top mass and effective coupling. This shows that the discovery potential reaches up to roughly 1400 GeV for the heavy top quark mass in regions of a still reliable heavy top quark coupling.

We encourage the experimental collaborations to look into this channel as a possible discovery channel as well as a means to get direct access to the mass of the heavy top with a final uncertainty of 75 GeV or better.

Acknowledgments

The authors of this paper are grateful for useful discussions with Maikel de Vries, Lorenzo Basso, Stefan Prestel, Fabian Bach, Diptimoy Ghosh, Piero Ferrarese. MT has been partially supported by the Deutsche Forschungsgemeinschaft within the Collaborative Research Center SFB 676 "Particles, Strings, Early Universe".

References

- [1] **CMS Collaboration**, S. Chatrchyan et al., *Observation of a new boson at a mass of 125 GeV with the CMS experiment at the LHC*, *Phys.Lett.* **B716** (2012) 30–61, [[arXiv:1207.7235](#)].
- [2] **ATLAS Collaboration**, G. Aad et al., *Observation of a new particle in the search for the Standard Model Higgs boson with the ATLAS detector at the LHC*, *Phys.Lett.* **B716** (2012) 1–29, [[arXiv:1207.7214](#)].
- [3] **ATLAS Collaboration**, *Search for pair and single production of new heavy quarks that decay to a Z boson and a third generation quark in pp collisions at $\sqrt{s} = 8$ TeV with the ATLAS detector*, tech. rep., ATLAS-CONF-2014-036, ATLAS-COM-CONF-2014-055, 2014.
- [4] **ATLAS Collaboration**, G. Aad et al., *Search for pair and single production of new heavy quarks that decay to a Z boson and a third-generation quark in pp collisions at $\sqrt{s} = 8$ TeV with the ATLAS detector*, [arXiv:1409.5500](#).
- [5] **ATLAS Collaboration**, *Search for pair production of heavy top-like quarks decaying to a high- p_T W boson and a b quark in the lepton plus jets final state in pp collisions at $\sqrt{s} = 8$ TeV with the ATLAS detector*, tech. rep., ATLAS-CONF-2013-060, ATLAS-COM-CONF-2013-066, 2013.
- [6] **CMS Collaboration**, *Boosted Top Jet Tagging at CMS*, tech. rep., CMS-PAS-JME-13-007, 2014.
- [7] **CMS Collaboration**, S. Chatrchyan et al., *Inclusive search for a vector-like T quark with charge $\frac{2}{3}$ in pp collisions at $\sqrt{s} = 8$ TeV*, *Phys.Lett.* **B729** (2014) 149–171, [[arXiv:1311.7667](#)].
- [8] **CMS Collaboration**, *Search for vector-like top quark partners produced in association with Higgs bosons in the diphoton final state*, tech. rep., CMS-PAS-B2G-14-003, 2014.

- [9] **CMS Collaboration**, *Search for top-Higgs resonances in all-hadronic final states using jet substructure methods*, tech. rep., CMS-PAS-B2G-14-002, 2014.
- [10] **CMS Collaboration**, *Search for Vector-Like b' Pair Production with Multilepton Final States in pp collisions at $\sqrt{s} = 8$ TeV*, tech. rep., CMS-PAS-B2G-13-003, 2013.
- [11] R. Contino and G. Servant, *Discovering the top partners at the LHC using same-sign dilepton final states*, *JHEP* **0806** (2008) 026, [[arXiv:0801.1679](#)].
- [12] J. Aguilar-Saavedra, *Identifying top partners at LHC*, *JHEP* **0911** (2009) 030, [[arXiv:0907.3155](#)].
- [13] J. Mrazek and A. Wulzer, *A Strong Sector at the LHC: Top Partners in Same-Sign Dileptons*, *Phys.Rev.* **D81** (2010) 075006, [[arXiv:0909.3977](#)].
- [14] S. Gopalakrishna, T. Mandal, S. Mitra, and R. Tibrewala, *LHC Signatures of a Vector-like b'* , *Phys.Rev.* **D84** (2011) 055001, [[arXiv:1107.4306](#)].
- [15] N. Vignaroli, *Early discovery of top partners and test of the Higgs nature*, *Phys.Rev.* **D86** (2012) 075017, [[arXiv:1207.0830](#)].
- [16] A. De Simone, O. Matsedonskyi, R. Rattazzi, and A. Wulzer, *A First Top Partner Hunter's Guide*, *JHEP* **1304** (2013) 004, [[arXiv:1211.5663](#)].
- [17] J. Kearney, A. Pierce, and J. Thaler, *Top Partner Probes of Extended Higgs Sectors*, *JHEP* **1308** (2013) 130, [[arXiv:1304.4233](#)].
- [18] S. Gopalakrishna, T. Mandal, S. Mitra, and G. Moreau, *LHC Signatures of Warped-space Vectorlike Quarks*, *JHEP* **1408** (2014) 079, [[arXiv:1306.2656](#)].
- [19] J. Li, D. Liu, and J. Shu, *Towards the fate of natural composite Higgs model through single t' search at the 8 TeV LHC*, *JHEP* **1311** (2013) 047, [[arXiv:1306.5841](#)].
- [20] A. Azatov, M. Salvarezza, M. Son, and M. Spannowsky, *Boosting Top Partner Searches in Composite Higgs Models*, *Phys.Rev.* **D89** (2014) 075001, [[arXiv:1308.6601](#)].
- [21] S. Beauceron, G. Cacciapaglia, A. Deandrea, and J. D. Ruiz-Alvarez, *Fully hadronic decays of a singly produced vector-like top partner at the LHC*, [arXiv:1401.5979](#).
- [22] N. G. Ortiz, J. Ferrando, D. Kar, and M. Spannowsky, *Reconstructing singly produced top partners in decays to Wb* , [arXiv:1403.7490](#).
- [23] C. Han, A. Kobakhidze, N. Liu, L. Wu, and B. Yang, *Constraining Top partner and Naturalness at the LHC and TLEP*, [arXiv:1405.1498](#).
- [24] G. Brooijmans, R. Contino, B. Fuks, F. Moortgat, P. Richardson, et al., *Les Houches 2013: Physics at TeV Colliders: New Physics Working Group Report*, [arXiv:1405.1617](#).
- [25] S. Yang, J. Jiang, Q.-S. Yan, and X. Zhao, *Hadronic b' search at the LHC with top and W taggers*, [arXiv:1405.2514](#).
- [26] M. Endo, K. Hamaguchi, K. Ishikawa, and M. Stoll, *Reconstruction of Vector-like Top Partner from Fully Hadronic Final States*, [arXiv:1405.2677](#).
- [27] B. Gripaios, T. Mueller, M. Parker, and D. Sutherland, *Search Strategies for Top Partners in Composite Higgs models*, [arXiv:1406.5957](#).
- [28] O. Matsedonskyi, G. Panico, and A. Wulzer, *On the Interpretation of Top Partners Searches*, [arXiv:1409.0100](#).

- [29] M. Backović, T. Flacke, S. J. Lee, and G. Perez, *LHC Top Partner Searches Beyond the 2 TeV Mass Region*, [arXiv:1409.0409](#).
- [30] L. Basso and J. Andrea, *Discovery potential for $T' \rightarrow tZ$ in the trilepton channel at the LHC*, [arXiv:1411.7587](#).
- [31] D. B. Kaplan and H. Georgi, *$SU(2) \times U(1)$ Breaking by Vacuum Misalignment*, *Phys.Lett.* **B136** (1984) 183.
- [32] D. B. Kaplan, H. Georgi, and S. Dimopoulos, *Composite Higgs Scalars*, *Phys.Lett.* **B136** (1984) 187.
- [33] D. B. Kaplan, *Flavor at SSC energies: A New mechanism for dynamically generated fermion masses*, *Nucl.Phys.* **B365** (1991) 259–278.
- [34] R. Contino, T. Kramer, M. Son, and R. Sundrum, *Warped/composite phenomenology simplified*, *JHEP* **0705** (2007) 074, [[hep-ph/0612180](#)].
- [35] K. Agashe, R. Contino, and A. Pomarol, *The Minimal composite Higgs model*, *Nucl.Phys.* **B719** (2005) 165–187, [[hep-ph/0412089](#)].
- [36] R. Contino, L. Da Rold, and A. Pomarol, *Light custodians in natural composite Higgs models*, *Phys.Rev.* **D75** (2007) 055014, [[hep-ph/0612048](#)].
- [37] M. S. Carena, E. Ponton, J. Santiago, and C. Wagner, *Electroweak constraints on warped models with custodial symmetry*, *Phys.Rev.* **D76** (2007) 035006, [[hep-ph/0701055](#)].
- [38] S. R. Coleman, J. Wess, and B. Zumino, *Structure of phenomenological Lagrangians. 1.*, *Phys.Rev.* **177** (1969) 2239–2247.
- [39] J. Callan, Curtis G., S. R. Coleman, J. Wess, and B. Zumino, *Structure of phenomenological Lagrangians. 2.*, *Phys.Rev.* **177** (1969) 2247–2250.
- [40] N. Arkani-Hamed, A. Cohen, E. Katz, and A. Nelson, *The Littlest Higgs*, *JHEP* **0207** (2002) 034, [[hep-ph/0206021](#)].
- [41] H.-C. Cheng and I. Low, *TeV symmetry and the little hierarchy problem*, *JHEP* **0309** (2003) 051, [[hep-ph/0308199](#)].
- [42] H.-C. Cheng and I. Low, *Little hierarchy, little Higgses, and a little symmetry*, *JHEP* **0408** (2004) 061, [[hep-ph/0405243](#)].
- [43] T. Han, H. E. Logan, B. McElrath, and L.-T. Wang, *Phenomenology of the little Higgs model*, *Phys.Rev.* **D67** (2003) 095004, [[hep-ph/0301040](#)].
- [44] J. Hubisz and P. Meade, *Phenomenology of the littlest Higgs with T-parity*, *Phys.Rev.* **D71** (2005) 035016, [[hep-ph/0411264](#)].
- [45] J. Hubisz, P. Meade, A. Noble, and M. Perelstein, *Electroweak precision constraints on the littlest Higgs model with T parity*, *JHEP* **0601** (2006) 135, [[hep-ph/0506042](#)].
- [46] C.-R. Chen, K. Tobe, and C.-P. Yuan, *Higgs boson production and decay in little Higgs models with T-parity*, *Phys.Lett.* **B640** (2006) 263–271, [[hep-ph/0602211](#)].
- [47] A. Belyaev, C.-R. Chen, K. Tobe, and C.-P. Yuan, *Phenomenology of littlest Higgs model with T-parity: including effects of T-odd fermions*, *Phys.Rev.* **D74** (2006) 115020, [[hep-ph/0609179](#)].
- [48] M. Blanke, A. J. Buras, A. Poschenrieder, S. Recksiegel, C. Tarantino, et al., *Rare and*

- CP-Violating K and B Decays in the Littlest Higgs Model with T-Parity*, *JHEP* **0701** (2007) 066, [[hep-ph/0610298](#)].
- [49] C. Csaki, J. Hubisz, G. D. Kribs, P. Meade, and J. Terning, *Big corrections from a little Higgs*, *Phys.Rev.* **D67** (2003) 115002, [[hep-ph/0211124](#)].
 - [50] W. Kilian and J. Reuter, *The Low-energy structure of little Higgs models*, *Phys.Rev.* **D70** (2004) 015004, [[hep-ph/0311095](#)].
 - [51] J. Reuter and M. Tonini, *Can the 125 GeV Higgs be the Little Higgs?*, *JHEP* **1302** (2013) 077, [[arXiv:1212.5930](#)].
 - [52] W. Kilian, D. Rainwater, and J. Reuter, *Pseudo-axions in little Higgs models*, *Phys.Rev.* **D71** (2005) 015008, [[hep-ph/0411213](#)].
 - [53] W. Kilian, D. Rainwater, and J. Reuter, *Distinguishing little-Higgs product and simple group models at the LHC and ILC*, *Phys.Rev.* **D74** (2006) 095003, [[hep-ph/0609119](#)].
 - [54] J. Berger, J. Hubisz, and M. Perelstein, *A Fermionic Top Partner: Naturalness and the LHC*, *JHEP* **1207** (2012) 016, [[arXiv:1205.0013](#)].
 - [55] M. Asano, S. Matsumoto, N. Okada, and Y. Okada, *Cosmic positron signature from dark matter in the littlest Higgs model with T-parity*, *Phys.Rev.* **D75** (2007) 063506, [[hep-ph/0602157](#)].
 - [56] J. Reuter, M. Tonini, and M. de Vries, *Little Higgs Model Limits from LHC - Input for Snowmass 2013*, [[arXiv:1307.5010](#)].
 - [57] J. Reuter, M. Tonini, and M. de Vries, *Littlest Higgs with T-parity: Status and Prospects*, *JHEP* **1402** (2014) 053, [[arXiv:1310.2918](#)].
 - [58] M. Buchkremer, G. Cacciapaglia, A. Deandrea, and L. Panizzi, *Model Independent Framework for Searches of Top Partners*, *Nucl.Phys.* **B876** (2013) 376–417, [[arXiv:1305.4172](#)].
 - [59] J. M. Butterworth, A. R. Davison, M. Rubin, and G. P. Salam, *Jet substructure as a new Higgs search channel at the LHC*, *Phys.Rev.Lett.* **100** (2008) 242001, [[arXiv:0802.2470](#)].
 - [60] T. Plehn, M. Spannowsky, M. Takeuchi, and D. Zerwas, *Stop Reconstruction with Tagged Tops*, *JHEP* **1010** (2010) 078, [[arXiv:1006.2833](#)].
 - [61] T. Plehn and M. Spannowsky, *Top Tagging*, *J.Phys.* **G39** (2012) 083001, [[arXiv:1112.4441](#)].
 - [62] J. Alwall, R. Frederix, S. Frixione, V. Hirschi, F. Maltoni, et al., *The automated computation of tree-level and next-to-leading order differential cross sections, and their matching to parton shower simulations*, [[arXiv:1405.0301](#)].
 - [63] T. Sjostrand, S. Mrenna, and P. Z. Skands, *A Brief Introduction to PYTHIA 8.1*, *Comput.Phys.Commun.* **178** (2008) 852–867, [[arXiv:0710.3820](#)].
 - [64] **DELPHES 3**, J. de Favereau et al., *DELPHES 3, A modular framework for fast simulation of a generic collider experiment*, *JHEP* **1402** (2014) 057, [[arXiv:1307.6346](#)].
 - [65] W. Kilian, T. Ohl, and J. Reuter, *WHIZARD: Simulating Multi-Particle Processes at LHC and ILC*, *Eur.Phys.J.* **C71** (2011) 1742, [[arXiv:0708.4233](#)].
 - [66] M. Moretti, T. Ohl, and J. Reuter, *O’Mega: An Optimizing matrix element generator*, [[hep-ph/0102195](#)].

- [67] W. Kilian, J. Reuter, S. Schmidt, and D. Wiesler, *An Analytic Initial-State Parton Shower*, *JHEP* **1204** (2012) 013, [[arXiv:1112.1039](#)].
- [68] M. Cacciari, G. P. Salam, and G. Soyez, *FastJet User Manual*, *Eur.Phys.J.* **C72** (2012) 1896, [[arXiv:1111.6097](#)].
- [69] M. Cacciari and G. P. Salam, *Dispelling the N^3 myth for the k_t jet-finder*, *Phys.Lett.* **B641** (2006) 57–61, [[hep-ph/0512210](#)].
- [70] N. D. Christensen and C. Duhr, *FeynRules - Feynman rules made easy*, *Comput.Phys.Commun.* **180** (2009) 1614–1641, [[arXiv:0806.4194](#)].
- [71] C. Degrande, C. Duhr, B. Fuks, D. Grellscheid, O. Mattelaer, et al., *UFO - The Universal FeynRules Output*, *Comput.Phys.Commun.* **183** (2012) 1201–1214, [[arXiv:1108.2040](#)].
- [72] N. D. Christensen, C. Duhr, B. Fuks, J. Reuter, and C. Speckner, *Introducing an interface between WHIZARD and FeynRules*, *Eur.Phys.J.* **C72** (2012) 1990, [[arXiv:1010.3251](#)].
- [73] M. Aliev, H. Lacker, U. Langenfeld, S. Moch, P. Uwer, et al., *HATHOR: HAdronic Top and Heavy quarks crOss section calculatoR*, *Comput.Phys.Commun.* **182** (2011) 1034–1046, [[arXiv:1007.1327](#)].
- [74] P. Kant, O. Kind, T. Kintscher, T. Lohse, T. Martini, et al., *HATHOR for single top-quark production: Updated predictions and uncertainty estimates for single top-quark production in hadronic collisions*, [arXiv:1406.4403](#).
- [75] S. Catani, F. Krauss, R. Kuhn, and B. Webber, *QCD matrix elements + parton showers*, *JHEP* **0111** (2001) 063, [[hep-ph/0109231](#)].
- [76] L. Loennblad, *Correcting the color dipole cascade model with fixed order matrix elements*, *JHEP* **0205** (2002) 046, [[hep-ph/0112284](#)].
- [77] L. Loennblad and S. Prestel, *Matching Tree-Level Matrix Elements with Interleaved Showers*, *JHEP* **1203** (2012) 019, [[arXiv:1109.4829](#)].
- [78] S. Catani, L. Cieri, G. Ferrera, D. de Florian, and M. Grazzini, *Vector boson production at hadron colliders: a fully exclusive QCD calculation at NNLO*, *Phys.Rev.Lett.* **103** (2009) 082001, [[arXiv:0903.2120](#)].
- [79] A. Kardos, Z. Trocsanyi, and C. Papadopoulos, *Top quark pair production in association with a Z-boson at NLO accuracy*, *Phys.Rev.* **D85** (2012) 054015, [[arXiv:1111.0610](#)].
- [80] J. Campbell, R. K. Ellis, and R. Roetsch, *Single top production in association with a Z boson at the LHC*, *Phys.Rev.* **D87** (2013), no. 11 114006, [[arXiv:1302.3856](#)].
- [81] **ATLAS Collaboration**, G. Aad et al., *Search for anomalous production of prompt like-sign lepton pairs at $\sqrt{s} = 7$ TeV with the ATLAS detector*, *JHEP* **1212** (2012) 007, [[arXiv:1210.4538](#)].
- [82] G. Choudalakis, *On hypothesis testing, trials factor, hypertexts and the BumpHunter*, [arXiv:1101.0390](#).